

# **Functionalized biodegradable co-polyesters for medical applications**

Maliheh Amini Moghaddam, Ph.D.

Doctoral Thesis Summary

Doctoral Thesis Summary

# **Functionalized biodegradable co-polyesters for medical applications**

**Funkcionalizované biologicky rozložitelné kopolyestery pro lékařské  
aplikace**

Author: **Maliheh Amini Moghaddam, Ph.D.**

Degree programme: P2808 Chemistry and Materials Technology

Degree course: 2808v006 Technology of Macromolecular Compounds

Supervisor: Prof. Ing. Vladimír Sedlařík, Ph.D.

External examiners: Prof. Mohamad Bakar, Ph.D., doc. Ing. Adriana Kolvalčík,  
Ph.D., Prof. Ing. Petr Slobodian, Ph.D.

Zlín, May-2021

© Maliheh Amini Moghaddam

Published by **Tomas Bata University in Zlín** in the Edition **Doctoral Thesis Summary**.

The publication was issued in the year 2021.

Key words: polyesters, *biodegradable polymers*, *medical application*, *modification*, *porous materials*, *polylactic acid*.

Klíčová slova: *polyester*, *biodegradovatelné polymery*, *aplikace v medicince*, *modifikace*, *porézní materiály*, *polylaktid*.

Full text of the doctoral thesis is available in the Library of TBU in Zlín

ISBN 978-80-7678-002-6

# TABLE OF CONTENT

ABSTRACT.....	6
ABSTRAKT.....	6
1. INTRODUCTION .....	7
AIMS OF WORK .....	8
2. EXPERIMENTAL PART .....	9
2.1. Preparation and characterization of microcellular antibacterial polylactide-based systems prepared by additive extrusion with ALUM .....	9
2.2. Preparation and characterization of polylactide-based porous systems mat for wound dressing application .....	21
SUMMARY OF WORK .....	33
REFERENCES.....	34
LIST OF FIGURES .....	38
LIST OF TABELS .....	39
CURRICULUM VITAE .....	40
LIST OF PUBLICATIONS .....	42

## **ACKNOWLEDGEMENTS**

With many thanks to my supervisor prof. Vladimír Sedlařík for his guidance during this research.

To all people from Tomas Bata University and people from my internship in Australia, Monash University who helped me during this journey.

To my parents and brothers, without their supports and everlasting encouragement, I could not have completed my Ph.D.

## **DEDICATION**

To my parents and my brothers.

To Ph.D. students in flight (ps752) who were unable to defend their doctoral dissertation. Rest in peace.

## **ABSTRACT**

This doctoral thesis is aimed at development and characterizations of novel biodegradable polylactid acid based systems for medical applications. The first part of this work is dedicated to preparation and characterization of novel biodegradable micro structured antibacterial systems where the antibacterial activity of the prepared materials was ensured by incorporation of the inorganic additive based on double sulfates of aluminium. The second part is focused on preparation and characterization of 3D polymer structures. The antibiotic gentamicin sulfate was used as model bioactive agent suitable for wound dressing applications. Both experimental parts were also comprised of the detailed structural and degradation studies that bring novel insights into the field of biodegradable polyesters medical research.

## **ABSTRAKT**

Tato disertační práce je zaměřena na vývoj a charakterizaci nových biologicky odbouratelných systémů na bázi kyseliny polymléčné pro lékařské aplikace. První část této práce je věnována přípravě a charakterizaci mikrostrukturovaných antibakteriálních systémů, kde byla antibakteriální aktivita připravených materiálů zprostředkována pomocí anorganického aditiva na bázi hlinitých podvojných solí kyseliny sírové. Druhá část je zaměřena na přípravu a charakterizaci 3D polymerních struktur pro krytí ran. Jako modelovou bioaktivní látku bylo použito antibiotikum gentamicin sulfát. Obě experimentální studie obsahují detailní popis strukturních a degradačních vlastností vyvinutých systémů a přináší tak nové poznatky do oblasti materiálového výzkumu biorozložitelných polyesterů pro medicínské aplikace.

# INTRUCTION

Aliphatic polyesters were firstly used in medical applications as sutures in 1971. Since then, research in biodegradable aliphatic polyesters has gained considerable attention due to the increasingly attractive biomedical, environmental, and agricultural applications [1]. Especially, biodegradable polyesters have highly desirable applications due to their biocompatibility, biodegradability and bioresorbability properties in biomedical areas, such as pharmaceutical industry and tissue engineering scaffolds. All these applications mainly rely on the fact that the polymers ultimately disappear after providing the desired functionalities. In this respect, the mechanism of polyesters' degradation and erosion in aqueous media has drawn great attention [2, 3]. Although, polyesters combine relatively intrinsic properties (as mentioned above) with easy synthetic methods and acceptable production costs, they often have poor mechanical and physical properties. Therefore, augmented mechanical and physical properties can be achieved by tailoring the chemistry of polyesters [4, 5]. Modification is one of the promising ways to enhance the mechanical properties and improve the capabilities of existing biodegradable polyesters for desired biomedical applications [4].

The presented thesis is devoted to the preparation of biodegradable aliphatic polyesters and biopolymers for biomedical applications. The first section summarizes the development of microcellular antibacterial polylactide-based systems prepared by additive extrusion with ALUM. The second section focuses on polylactide-polyvinyl alcohol-based porous systems loaded with gentamicin for wound dressing applications.



## **AIMS OF WORK**

Aliphatic polyesters combine the rarely met properties of biocompatibility, bioresorbability, and biodegradability, which accounts for their broad use as biomaterials and as environmentally friendly thermoplastics. However, the lack of functional groups along the backbone and poor mechanical properties induce an intense limitation to extend new applications. It is highly desirable to implement efficient processes in order to modify biodegradable polyesters and tailor properties including crystallinity, hydrophilicity, and biodegradation rate. Therefore, the aim of the doctoral thesis is based on the state of the art study, and conclusions resulting from that are the following:

- Preparation and characterization of microcellular antibacterial poly lactide-based systems prepared by additive extrusion with ALUM.
- Poly lactide-polyvinyl alcohol-based porous systems loaded with gentamicin for wound dressing applications.

## 2. EXPERIMENTAL PART

### 2.1. Preparation and characterization of microcellular antibacterial polylactide-based systems prepared by additive extrusion with ALUM

#### Preparation of PLA mixtures

Prior to being compounded, PLA pellets were dried at 80°C under reduced pressure (300 mbar) for at least 8 hours. A co-rotating twin screw micro compounder (HAAKE MiniLab II, Thermo Scientific, Waltham, Massachusetts) which was equipped with two stainless steel screws and a bypass valve was utilized. This allowed continuous recirculation of the material at 190°C; with the screw speed set to 50 rpm for compounding operations without the bypass valve. The compositions of the resultant samples are shown in Table. 1.

Table. 1. Compositions of the investigated samples

<b>Component content (wt.%)/sample designation</b>	<b>PLA</b>	<b>ALUM</b>	<b>MSS</b>
PLA	100	-	-
PLA/ALUM	99	1	-
PLA/ALUM/MSS3	97	1	3
PLA/ALUM/MSS5	94	1	5
PLA/MSS3	97	-	3
PLA/MSS5	95	-	5

#### Results and discussions

##### Characterization of materials

Materials properties including molecular weight, thermal and mechanical properties and morphology of specimens prepared from neat PLA and microcellular PLA expanded by sodium bicarbonate and Alum as antimicrobial compound were investigated. Recognized as being environmentally friendly and cheap CBA, MSS decomposes at low temperature and releases CO<sub>2</sub> easily. Antibacterial modification was mediated by another inexpensive and widely available additive, ALUM. Papers in the literature highlight that PLA degrades during melting process methods such as extrusion [6], a phenomenon that could be accelerated by enhancing the material with additives [7, 8]. Therefore, the effect of agents on the properties of the PLA was

researched after the preparation process had ended, and these findings were compared with characteristics prior to commencement of said process.

## **Morphology**

Scanning electron microscopy (SEM) was utilized to investigate the morphology of samples, especially to gain data on the microstructure of the microcellular specimens. As can be observed from Figure 1, adding ALUM to neat PLA caused the specimens to develop more fracture-like characteristics than evidenced in neat PLA. As expected, the gases formed by the decomposition of MSS in the PLA during extrusion gave rise to an expanded pore structure in the majority of pores, measuring in the order of hundreds of micrometers. The higher expansion ratio and density discerned of the pores were achieved by employing a greater amount of the blowing agent: (5 wt% of MSS) in the samples PLA/MSS5 (Figure 1D) and PLA/ALUM/MSS5 (Figure 1F). Additionally, incorporating ALUM and combining it with the expansion process induced by the greater concentration of MSS led to decrease in cell size and increase in the cell density of the polymer matrix, in comparison with the PLA/MSS5 sample; notably, a more uniform cell structure was also obtained. The pores in the PLA/ALUM/MSS5 specimen were roughly comparable in size with the morphological characteristics of a microcellular PLA reported in a study [9], which had been formed by nitrogen in a supercritical state through injection molding experiments.

Table 2 summarizes the percentage of porosity of the microcellular PLA samples. In accordance with findings from the SEM images, free space volume was at its highest level when the greater concentration of MSS was utilized. Nevertheless, if applied in tandem with ALUM, porosity significantly diminished because of the less porous substructures formed, in addition to which the average pore size of the specimens reduced. These phenomena had been anticipated because of the number of bubbles nucleated, which is fully dependent on the concentration of the blowing agent dissolved in the polymer matrix [10].

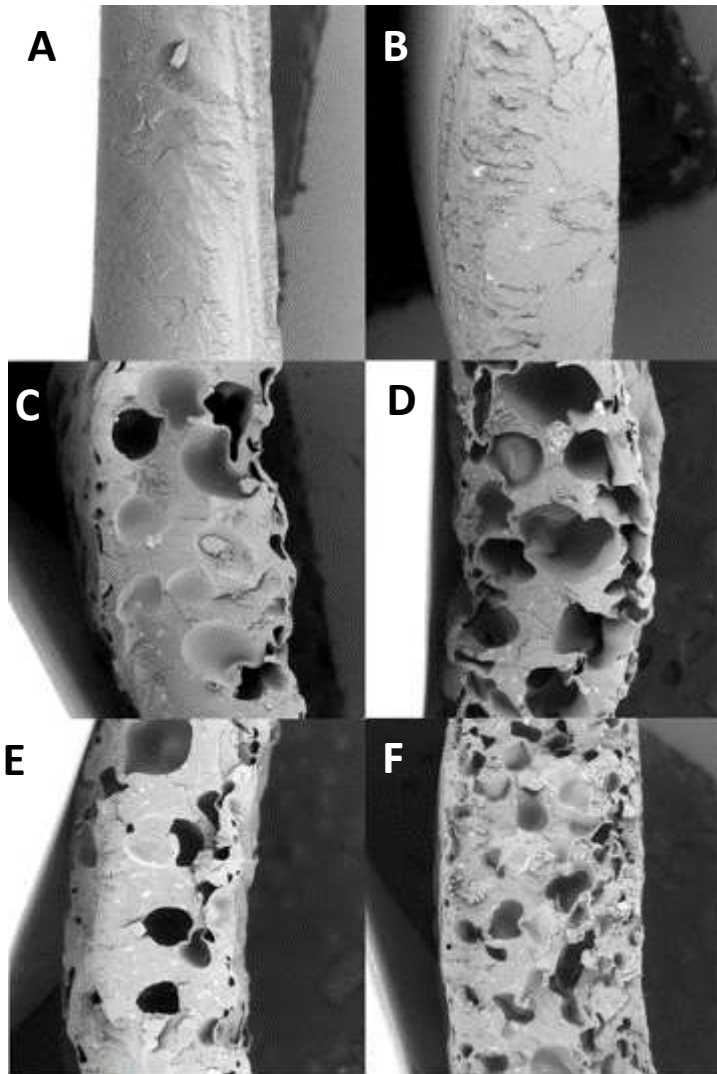


*Figure 1. SEM micrographs of the microstructures of (A) PLA, (B) PLA-ALUM, (C) PLA/MSS3, (D) PLA/MSS5, (E) PLA/ALUM/MSS3, (F) PLA/ALUM/MSS5.*

### **Molecular weight and distribution**

The average molecular weights of all samples, measured by GPC, are listed in Table. 2. Neat, unprocessed PLA was used as a reference to compare the results obtained for the final samples. As can be seen, a significant drop in Mw was detected for neat PLA after it had been processed in comparison with the same unprocessed material, caused by thermal degradation. This decline in Mw was much more pronounced for the material incorporating the antimicrobial agent ALUM and the composites expanded by MSS (PLA/ALUM, PLA/ALUM/MSS3,

PLA/ALUM/MSS5). The Mw of the neat PLA and PLA with additives dropped by approximately 14% and 43%, respectively, after processing the same.

Potentially, this significant reduction in Mw could be attributed to the acidic nature of ALUM ( $\text{KAl}(\text{SO}_4)\cdot 12\text{H}_2\text{O}$ ) and MSS, which were employed in tandem with the expansion agent. These additives act as an acidic catalyst, accelerating the random hydrolysis of the ester bonds in the PLA [11]. Furthermore, water molecules present in the chemical structure of ALUM could promote hydrolysis of the polymer. The concurrent effect exerted by the additives on acceleration of degradation is clearly evidenced in the Mw of the PLA/ALUM/MSS5 material, which contained ALUM and the greatest amount of the blowing agent

### **Thermal properties**

The results of DSC analysis, which are detailed in Table 2, demonstrate that the additives employed to prepare the antimicrobial microcellular PLA did not significantly influence the thermal properties of the given PLA, in comparison with the neat material prior to and after processing. The degree of crystallinity of the specimens, calculated from data obtained by thermal analysis, was very low. This can be attributed to the short time available for crystallization to occur during the preparation of the specimens. However, the slightly higher crystallinity of the PLA with additives potentially indicates their nucleation effect, facilitating PLA crystallization [12].

Table. 2. Selected material-related properties of samples after preparation and before degradation experiments.

Sample/property	Neat PLA prior to processing	Neat PLA after processing	PLA ALUM	PLA/MSS3	PLA/MSS5	PLA ALUM MSS3	PLA ALUM MSS5
Content of ALUM [%]	-	-	1	-	-	1	1
Content of BS [%]	-	-	-	3	5	3	5
$M_w^a$ [kg·mol <sup>-1</sup> ]	122.9	107.1	86.5	90.1	90.1	91.5	85.5
$\bar{D}^b$	2.44	2.12	2.43	2.53	2.42	2.34	2.24
$T_m^c$ [°C]	154.1	152.5	153.5	155.0	154.6	154.3	154.0
$\Delta H_m^d$ [J·g <sup>-1</sup> ]	-35.9	-26.9	-24.3	16.1	-27.7	-25.3	-27.8
$T_c^e$ [°C]	-	123.2	123.5	126.2	125.7	126.2	124.5
$\Delta H_c^f$ [J·g <sup>-1</sup> ]	-	26.2	22.0	16.6	24.5	21.1	25.0
$T_g^g$ [°C]	59.8	59.3	59.8	58.4	57.8	59.7	59.8
$\chi_c^h$ [%]	38.6	0.7	2.5	0.5	3.5	4.5	3.0
Porosity	-	-	-	22.9	29.8	19.1	17.9

<sup>a</sup> weight average molecular weight; <sup>b</sup> molar mass dispersity; <sup>c</sup> melting temperature; <sup>d</sup> enthalpies of melting; <sup>e</sup> crystallization temperature; <sup>d</sup> enthalpies of crystallization; <sup>g</sup> glass transition temperature; <sup>h</sup> calculated crystallinity; <sup>i</sup> neat PLA processed under identical conditions to the corresponding blends; <sup>j</sup> value obtained from DMA measurements.

## Mechanical properties

Tensile tests were conducted to determine the effect of the additives on mechanical properties of the samples. Table. 3. details the tensile strength, elongation at break and Young modulus of the pure PLA and PLA base samples. Supplementing neat PLA with ALUM subtly enhanced all the mechanical characteristics of the material. As anticipated, the mechanical properties of the expanded samples diminished significantly in a very similar manner, regardless of their exact composition. This

decline was more pronounced than the results published elsewhere [9], which investigated the comparable morphology of microcellular PLA specimens. Such a deterioration occurred primarily because of the free-space volume contained in the expanded samples, thereby deteriorating the integrity of the same, partially reducing their molecular weight and diminishing the resultant mechanical properties

Table. 3. Initial mechanical properties of neat PLA and microcellular PLA.

<b>Sample</b>	<b>Tensile strength (MPa)</b>	<b>Elongation at break (%)</b>	<b>Young's modulus (MPa)</b>
<b>Neat PLA after processing</b>	50.5 ± 2.6	16.7 ± 2.1	788.8 ± 62.9
<b>PLA-ALUM</b>	60.6 ± 2.6	16.8 ± 0.6	907.4 ± 88.1
<b>PLA/MSS3</b>	27.1 ± 0.6	10.2 ± 0.5	382.2 ± 34.3
<b>PLA/MSS5</b>	21.4 ± 0.8	8.2 ± 0.2	321.8 ± 80.0
<b>PLA/ALUM/MSS3</b>	20.9 ± 0.7	9.2 ± 0.7	345.6 ± 67.6
<b>PLA/ALUM/MSS5</b>	21.1 ± 1.0	7.3 ± 0.2	569.2 ± 25.5

## Hydrolysis

The effects of the additives and microcellular structure on the rate of hydrolysis of the PLA-based materials were investigated by GPC and DSC in an aqueous environment at 37°C in the presence of a microbial growth inhibiting substance (NaN<sub>3</sub>).

## Changes in molecular weight during abiotic degradation

GPC measurement was carried out to discern changes in the PLA at a molecular level during hydrolysis (Figure 2). Reductions in Mw occurred because of random chain scission of the ester bonds, an action that participated in such hydrolysis [13]. The Mw reduction rate in the neat PLA was in agreement with a previous investigation [13], which was performed at a temperature beneath the point of glass transition. At this temperature, when PLA is in the glassy state, the polymer chains are tightly bound to one another resulting in a limited mobility. Therefore, making it

much harder for water to penetrate the polymer matrix. Moreover, the kinetics or hydrolytic scission of ester bonds by water are reduced significantly. Herein, the microcellular materials (PLA/MSS3 and PLA/MSS5) showed a slightly accelerated chain scission rate than the neat PLA. This acceleration can be attributed to two factors: the lower  $M_w$  in the microcellular samples at the beginning of hydrolysis and their porous structure enabling effective contact of the polymer material with the degradation media. As a result, there was an increase in the effective surface area of the samples, allowing water to penetrate the polymer more readily than in the neat PLA. Interestingly, the  $M_w$  of samples incorporated with ALUM remained largely unchanged for about 30 days, after which it decreased at a similar rate as the material without the additive. Hence, although the microcellular samples reached a lower  $M_w$  at the end of the observation period of 140 days, the rate of hydrolysis of the microcellular specimens was somewhat comparable with that of the non-expanded PLA material.

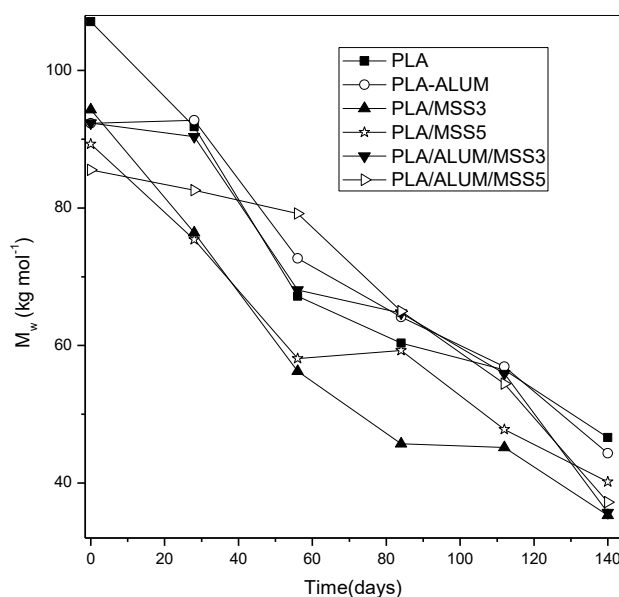


*Figure. 2. Molecular weight evolution of the materials during abiotic hydrolysis*

### **Changes in thermal properties during abiotic degradation**

Table. 4. illustrates the effect of abiotic hydrolysis (at 0.1 mol L<sup>-1</sup>, pH 7) on the thermal properties of the microcellular samples and contrasts them with those of the nonporous materials. The samples were initially highly amorphous [14, 15], but after 12 weeks, a visible increase in crystallinity was detected in the microcellular samples only. This indicated that some newly formed degradation products possessed



sufficient mobility to produce a crystalline lattice [14]. Notably, PLA/MSS5 showed the highest value for the degree of crystallinity, potentially attributable to the highly porous structure of the specimens. The formation of low-molecular-weight fragments, caused by chain scission of the ester bonds entrapped in the polymer matrix, brought about slight reduction in melting and glass transition temperatures. The new oligomers acted as a plasticizer, sufficiently lowering values for T<sub>g</sub> [13]. This behavior was again more pronounced for the microcellular samples, which was in agreement with the findings obtained from GPC analysis. A split in the melting peak also appeared at certain sampling times for all the specimens. In the nonporous samples, this could be attributed to a different rate of chain scission in the cortex of the material, while in the microcellular specimens, the reason is selective degradation of the amorphous phase rather than the crystalline part.

Table. 4. Thermal properties of samples prior to and after abiotic hydrolysis at various times.

<b>Sample</b>	<b>Time of hydrolysis (weeks)</b>	<b>T<sub>m_1</sub><sup>a</sup> [°C]</b>	<b>ΔH<sub>m_1</sub><sup>b</sup> [J·g<sup>-1</sup>]</b>	<b>T<sub>m_2</sub><sup>c</sup> [°C]</b>	<b>ΔH<sub>m_c</sub><sup>d</sup></b>	<b>T<sub>c</sub><sup>e</sup> [°C]</b>	<b>ΔH<sub>c</sub><sup>f</sup> [J·g<sup>-1</sup>]</b>	<b>T<sub>g</sub><sup>g</sup> [°C]</b>	<b>χ<sub>c</sub><sup>h</sup> [%]</b>
<b>PLA</b>	0	152.5	-	-	-26.9	123.2	26.2	59.3	0.7
	4	152.2	-	-	-35.9	119.2	34.5	60.0	1.5
	12	149.0	-22.4	156.5	-39.4	110.5	37.9	59.4	1.6
	20	148.1	-14.6	157.3	-40.3	104.6	40.1	58.7	0.2
<b>PLA-ALUM</b>	0	153.5	-	-	-24.3	123.5	22.0	59.8	2.5
	4	152.0	-	-	-33.0	117.7	31.0	59.2	2.2
	12	148.9	-19.7	156.5	-38.6	109.0	33.6	59.29	5.4
	20	148.1	-15.4	157.0	-42.5	105.1	37.7	58.93	5.2
<b>PLA/MSS3</b>	0	155.0	-	-	-16.1	126.2	16.6	58.4	0.5
	4	151.1	-24.01	157.4	-36.3	114.7	34.18	59.1	2.3
	12	148.9	-12.33	156.8	-38.5	107.7	30.3	59.1	8.7
	20	155.1	-	-	-41.5	95.4	28.1	56.5	14.4
<b>PLA/MSS5</b>	0	154.6	-	-	-27.7	125.7	24.5	57.8	3.5

	4	152.2	-16.2	158.7	-30.6	114.8	26.2	60.6	4.8
	12	148.6	-17.8	157.1	-41.8	107.7	31.5	58.7	11.1
	20	146.9	-11.0	155.8	-42.8	99.7	28.8	57.7	15.0
<b>PLA/ALUM/MSS3</b>	0	154.3	-	-	-25.3	126.2	21.1	59.7	4.5
	4	151.3	-28.1	157.5	-42.7	119.8	39.7	59.3	3.3
	12	148.9	-12.7	157.3	-38.0	106.5	28.7	58.8	10.0
	20	154.5	-	-	-42.3	94.0	33.4	56.2	9.6
<b>PLA/ALUM/MSS5</b>	0	154.0	-	-	-27.8	124.5	25.0	59.8	3.0
	4	152.2	-	155.7	-33.3	117.7	25.3	59.4	8.6
	12	155.8	-	-	-37.9	103.5	22.6	57.6	16.4
	20	155.7	-	-	-41.8	952	31.9	56.1	10.7

<sup>a</sup> melting temperature of first peak; <sup>b</sup> enthalpies of melting of first peak; <sup>c</sup> melting temperature of second peak; <sup>d</sup> total enthalpies of melting; <sup>e</sup> crystallization temperature; <sup>f</sup> enthalpies of crystallization; <sup>g</sup> glass transition temperature; <sup>h</sup> calculated crystallinity;

### Release of the antimicrobial compound

Release of the antimicrobial agent from the PLA samples in phosphate buffer solution (pH = 7.4) was investigated to evaluate the effect of the porous structures on the stability of ALUM in the polymer matrix. Samples containing ALUM were incubated at 37 °C for approximately 120 days in the buffer solution. The release of ALUM occurred by the microcellular samples (PLA/ALUM/MSS). Initial rapid release occurred around 10 days and followed by a gradual release. The initial release can be attributed to the release of ALUM located close to the surface. In contrast, nonporous samples exhibited a rapid release of less than 1% of the ALUM over a few days, followed by negligible release in the subsequent period (Figure 3). The more rapid release observed from the porous samples could be attributed to the microcellular morphology of the samples, which possess the larger active surface area; this permits faster penetration of water into the polymer matrix and subsequent diffusion of ALUM onto the polymer surface. Comparing the two porous samples revealed that the initial rapid release of both was almost identical, although the release of ALUM during the following phase was slightly more pronounced for PLA/ALUM/MSS5, as it contained smaller and more numerous pores in its structure.

At the end of the observation period, the cumulative release of ALUM equalled approximately 15% and 10% for PLA/ALUM/MSS5 and PLA/ALUM/MSS3, respectively, whereas for PLA-ALUM, it was only about 1%.

In point of fact, while the release of an antimicrobial agent from a medical implant might diminish the antimicrobial effect of the given material, it could still prevent microbial growth in its surroundings. Note that the tolerance of PLA/ALUM was very low, hence not visible in Figure 3.

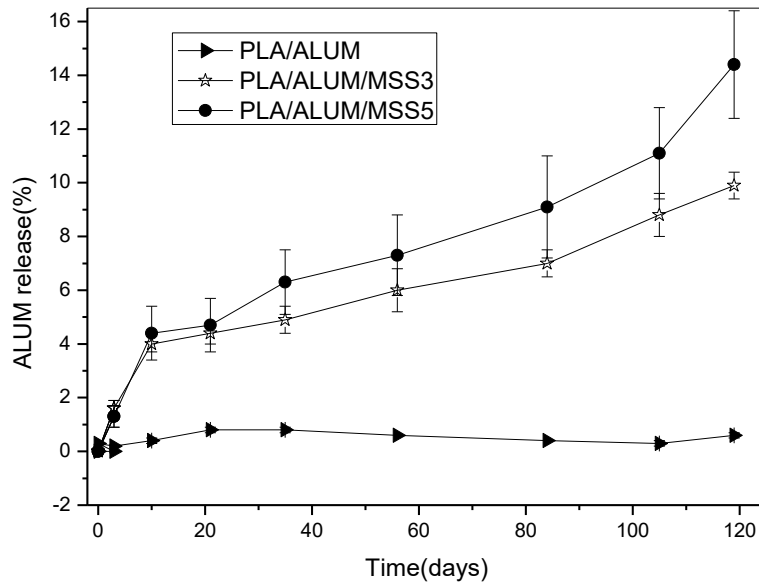


Figure. 3. Release of ALUM in phosphate buffer saline (PBS) buffer (pH = 7.4) at 37°C.

### Antimicrobial properties

In order to inhibit microorganism growth effectively, their life cycle has to be interrupted. Table. 5 shows the reduction in bacterial growth of *S. aureus* (gram-positive) and *E. coli* (gram-negative) on the surface of the PLA-ALUM, microcellular PLA/ALUM/MSS3, and microcellular PLA/ALUM/MSS5 specimens after 24 hours of incubation at  $35 \pm 2$  °C. In general, PLA-ALUM specimens showed no alteration in bacterial growth. Whereas, microcellular specimens showed promising results at inhibiting the growth of the tested bacterial strains. As can be seen in the table ALUM shows effective antimicrobial activity against the gram-negative bacteria (*E. coli*), as compared to a gram-positive (*S. aureus*). Gupta et al, reported that ALUM could be considered an effective antimicrobial agent against the

gram-negative bacteria, in comparison with a gram-positive. This phenomenon occurs because of the differences in the membrane structure and thickness of the peptidoglycan layer in gram-positive and gram-negative microorganisms [16-19]. Some studies reported that MSS showed antimicrobial activity against *E. coli* and *S. aureus*; therein, the value of CR rose as a consequence of increasing the amount of MSS [20]. This means that synergic effects could be expected from ALUM and MSS. Surprisingly, only PLA/ALUM/MSS5 showed a noticeable drop in reduction of CFU (CR) against *E. coli*. This can be attributed to smaller and more numerous pores of the specimens that may affect the results of the applied testing procedure (ISO 22196). However, the obtained results showed antibacterial effects of both PLA/ALUM/MSS3 and PLA/ALUM/MSS5 samples

Table. 5. Reduction in colony forming units (CR) effected by of pure PLA-ALUM, microcellular PLA/ALUM/MSS3, and microcellular PLA/ALUM/MSS5

<b>sample</b>	<b>CR (%)</b>	<b>CR (%)</b>
	<b><i>E. coli</i> CCM 4517</b>	<b><i>S. aureus</i> CCM 4516</b>
<b>PLA-ALUM</b>	100	100
<b>PLA/ALUM/MSS3</b>	93	98
<b>PLA/ALUM/MSS5</b>	64	97

## CONCLUSION

This work focused on preparing and characterizing of antibacterial, microcellular polymeric material based on PLA, utilizing potassium aluminum sulfate dodecahydrate (ALUM) as an antimicrobial agent and monobasic sodium salts as a blowing agent. Morphological analysis of the surface of specimens revealed that adding ALUM instigated greater cell density in the polymer matrix and reduced average cell size. Tests demonstrated that mechanical properties of microcellular PLA were diminished because of microcellular morphology, and hydrolysis acceleration took place due to increasing the effective surface area of the microcellular PLA, thereby evidencing a rapid reduction in molecular weight by approximately 43% in comparison with neat PLA. The microcellular PLA samples exhibited accelerated degradation, primarily due to their microcellular structure, facilitating better penetration of the buffer solution into the structure of samples. Furthermore, the release of an antimicrobial compound and subsequent antimicrobial activity against *S. aureus* and *E. coli* were evaluated. It was confirmed that the rate of release in PLA/ALUM/MSS5 (15 %) was higher than in other samples (10 %,

PLA/ALUM/MSS3), as a consequence of its microcellular morphology and more numerous pores in its structure. Finally, it was demonstrated that ALUM proved effective antimicrobial activity against the gram-positive and gram-negative bacteria utilized, although its effect was greater against the latter of the two.

## 2.2. Preparation and characterization of polylactide-based porous systems mat for wound dressing application

### Preparation of the porous mats

The organic phase was 2% PLA in chloroform solution and the aqueous phase was 0.1% PVA aqueous solution. Different salt concentrations were added to the aqueous phase (10 g/L NaCl and 0.4 mg/L KMnO<sub>4</sub>). The resultant organic solution was sprayed onto the PVA aqueous solution at the rate of 4 mL/min under moderate magnetic stirring (600 rpm) and 1 bar air-pressure at room temperature to form an oil in water (O/W) emulsion. Subsequently, stirring was maintained overnight in order to evaporate the chloroform. Next, the product was washed three times with deionized water (DI) and filtered. The loading of GS was performed by dissolving GS in DI water and dispersing the filtered product into the solution of GS and DI water. The final product was then frozen. In the final step, the frozen sample was lyophilized. Figure 4 shows the schematic diagram of the surface liquid spraying process.

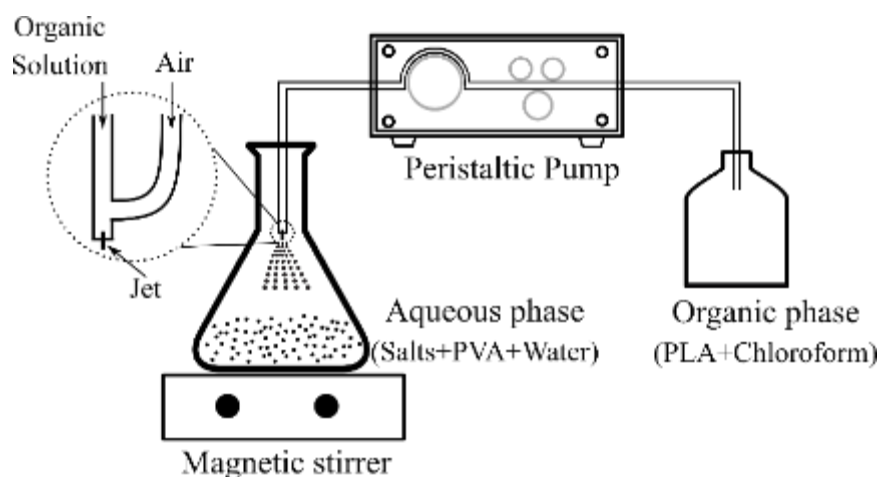


Figure. 4. Scheme of Surface liquid spraying process.

### Thermal treatment of the porous mats

In order to study the effect of thermal treatment, the porous mats were placed in an oven (Memmert, Germany) at 80°C for 2 minutes. The mats were then kept in the silica gel containing desiccator. Subsequently, thermal treated mats were then subjected to the various characterization tests as described below.

## Results and discussion

### Attenuated Total Reflection Fourier-transform infrared (ATR-FTIR) spectroscopy

The ATR-FTIR spectroscopy analysis was carried out to investigate the structural changes of mats based on PLA, PVA, and different salts before and after thermal treatment at the molecular level. The FT-IR spectra of mats are shown in Figure. 5. The PLA-PVA mats show some characteristic peaks identified by the strong infrared absorption band in the region of 1650–1754  $\text{cm}^{-1}$ , which corresponds to the stretching vibration of the carbon-oxygen double bond. The band at 1187  $\text{cm}^{-1}$  is assigned to the stretching vibration of the carbon-oxygen bond. The two peaks around 1448 and 1373  $\text{cm}^{-1}$  correspond to the methyl groups of the PLA-PVA mats. Moreover, the high intensive peak that is positioned at 3399  $\text{cm}^{-1}$  corresponds to the stretching vibration of the oxygen-hydrogen bond[21-23]. Figure. 5. illustrates that the intensity and position of the absorption peak of the hydroxyl group changed with the addition of salts and the thermal treatment. Addition of  $\text{KMnO}_4$  to the mat caused the disappearance of the OH peak in the FT-IR spectra, which indicates the oxidation of PVA to polyvinyl ketone (PVK). The formation of corresponding ketone is due to the fact that  $\text{KMnO}_4$  is a strong oxidizing agent[24-26].

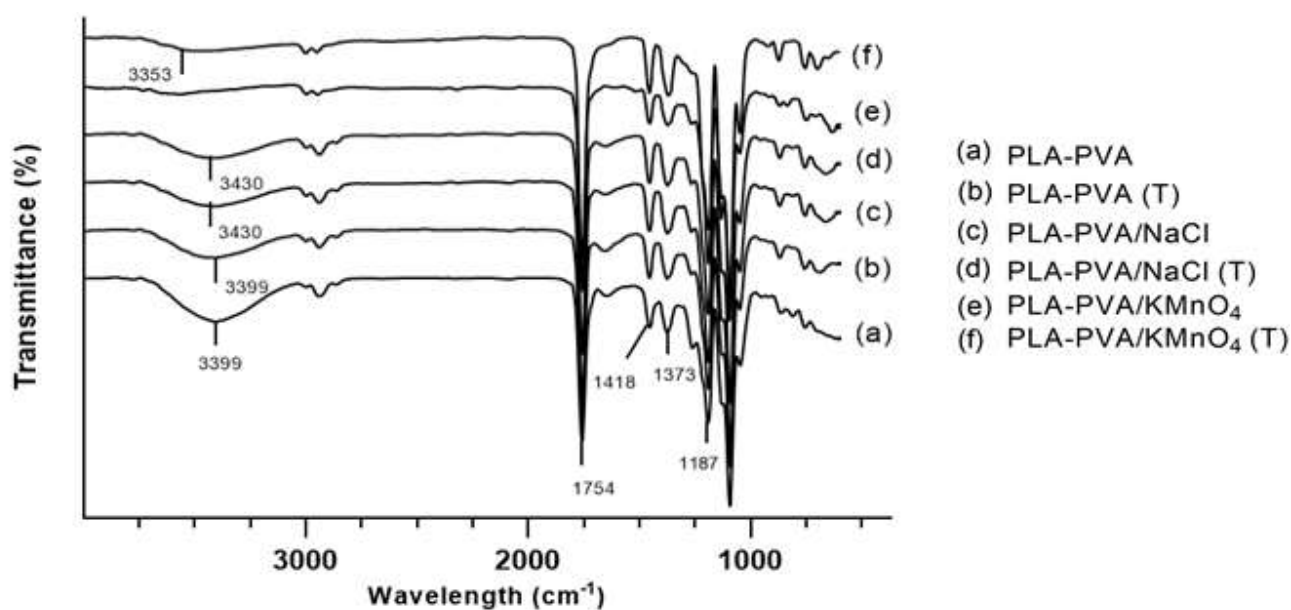


Figure. 5. FT-IR spectra of PLA-PVA (a), PLA-PVA (T) (b), PLA-PVA/ $\text{KMnO}_4$  (c), PLA-PVA/ $\text{KMnO}_4$  (T) (d), PLA-PV/ $\text{NaCl}$  (e), PLA-PVA/ $\text{NaCl}$  (T) (f) mats.

In the case of the addition of NaCl, the hydroxyl peak in PLA-PVA/NaCl mat is weaker than it is in PLA-PVA mat and its position was shifted slightly toward a higher frequency (3430 cm<sup>-1</sup>). This can be attributed to a higher degree of hydrogen bonding in the PLA-PVA mat, because hydrogen bonding is disrupted by the addition of NaCl [27]. The thermal treated PLA-PVA and PLA-PVA/NaCl mats show that the hydroxyl peak has a lower intensity in comparison with the non-thermal treated mats[28]. In case of the thermal treated PLA-PVA/KMnO<sub>4</sub> mat, the OH peak in the FT-IR spectra appear and it is shifted to a higher wavelength from (3353 cm<sup>-1</sup>). This can be explained by the partially formation of the carboxylic acid group due to the elevated temperature in the presence of KMnO<sub>4</sub> [29, 30].

### Thermal properties

DSC analysis of the porous mats was carried out to study the effects of the thermal treatment and salts on the thermal behavior of the mats. The correlated thermal properties of the mats are summarized in Table. 6. As expected, crystallinity ( $\chi_c$ ) increased after the thermal treatment of the mats[31]. The T<sub>g</sub> of the mats did not demonstrate any significant changes after the thermal treatment as shown in Figure. 6. Furthermore, T<sub>m</sub>, and T<sub>c</sub> values were not affected by the thermal treatment and were in agreement with the published literature values [31, 32]. Increase in the concentration of NaCl caused significant reduction in crystallinity, which could be attributed to the fact that high NaCl content impedes PLA chain mobility and thereby prohibits crystallization[33]. According to the literature, the oxidation of PLA and PVA by KMnO<sub>4</sub> caused a decrease in crystallinity [34, 35]. Moreover, the addition of salts induced a decrease in T<sub>c</sub>, an increase in T<sub>m</sub> (consistent with the results given in[36]), and showed no difference in the T<sub>g</sub> values.

Table. 6. Selected material-related properties of the mats before and after thermal treatment.

Sample/property	Untreated			After thermal treatment		
	PLA-PVA	PLA-PVA/KMnO <sub>4</sub>	PLA-PVA/NaCl	PLA-PVA	PLA-PVA/KMnO <sub>4</sub>	PLA-PVA/NaCl
$\chi_c$	5.1	4.9	0.7	8.8	5.3	3.0
T <sub>g</sub>	61.9	62.0	62.0	61.1	61.7	61.2
T <sub>c</sub>	129.9	118.3	115.4	130.4	118.1	114.4
T <sub>m</sub>	164.3	167.4	168.0	164.6	167.5	167.0



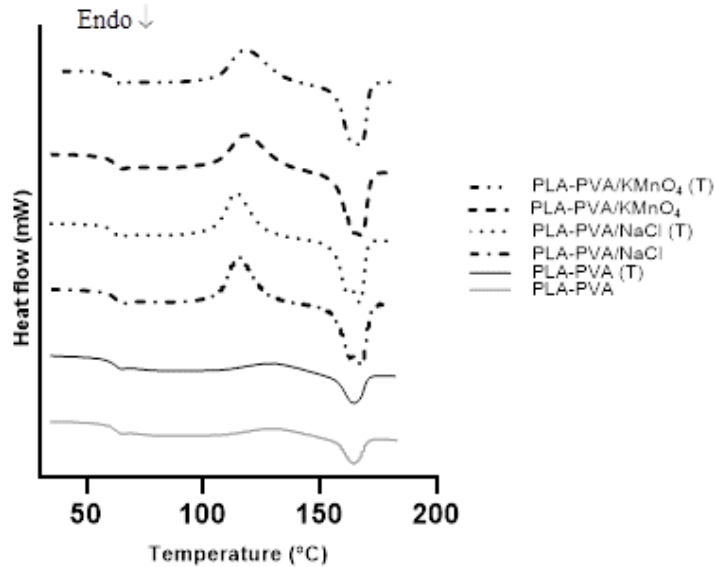


Figure. 6. DSC curves of porous PLA mats.

### Measurement of porosity

The study of the porosity of wound dressing is a very important factor as it affects the absorption capacity of exudates from the wound, which can reduce the probability of infection[37]. As shown in Table. 7, all the mats showed a porosity ranging between 68 - 94 %. These results indicate that the porosity was increased with the addition of the salts. A higher salt concentration led to increase in the porous structure, resulting in an irregular and spongier shape[38]. However, the total porosity of the mats slightly decreased after the thermal treatment[39-41]. The graph clearly shows that non-thermal treated mats with the highest concentration (10 g/L) of NaCl possessed the highest porosity (94%), whereas there was a reduction of porosity (92%) for thermal treated mat with the same concentration of NaCl. Addition of KMnO<sub>4</sub> to the mat also followed the same trend as NaCl in terms of porosity. It is worth noting that the thermal treated mat without salt (neat mat) showed the lowest levels of porosity (68%).

Table. 7. Porosity measurements of porous mats after 24 h of immersion in ethanol at room temperature.

	Untreated			After thermal treatment		
Sample	PLA-PVA	PLA-PVA/KMnO <sub>4</sub>	PLA-PVA/NaCl	PLA-PVA	PLA-PVA/KMnO <sub>4</sub>	PLA-PVA/NaCl
Porosity	69.87±2.1	78.77±4.2	94.1±1.5	68.1±1.2	75±0.94	92.86±0.54

### Morphology of the porous mats

The optical photographs PLA-PVA porous mat is shown in Figure. 7. PLA-PVA has white appearance with a smooth surface. Scanning electron microscopy (SEM) was used to investigate the effects of the addition of salts and thermal treatment on the morphology of porous mats. As can be observed from Figure. 8, the PLA-PVA mat show a disordered, interconnected pore-like structure with a rough surface. However, high resolution SEM analysis shows (Figure. 9 (a)) that the neat PLA-PVA mat, has fracture-like characteristics with almost no holes or pores. The addition of 10 g/L NaCl to the mats led to formation of more porous structures with interconnected pores with varying pore size in the range of 0.2 - 7  $\mu\text{m}$  (Figure. 9 (b)). As can be seen from Figure. 9 (c), the addition of 0.4 mg/L KMnO<sub>4</sub> to the mat led to formation of a porous structure in a range of 0.4 - 4  $\mu\text{m}$ . However, comparing Figures 9 (b) and 9 (c) leads to two main observations: (1) the addition of 10 g/L NaCl to the mats led to formation of more porous structures compared to the addition of 0.4 mg/L KMnO<sub>4</sub> to the mats; and (2) the addition of different salts leads to the formation of different shapes and sizes of the pores. It is likely that the size and shape of the pores are different due to the oxidation of PVA by KMnO<sub>4</sub> (discussed in FT-IR analysis section) in the case of PLA-PVA/KMnO<sub>4</sub>. Pore formation of the mats containing salts can be attributed to its osmotic properties in aqueous phase, which has already been demonstrated by other authors[38, 42]. The mats that have been subjected to thermal treatment present smoother surfaces with fewer fractures and less porosity (Figure. 9). These results were consistent with other studies[40, 41].



Figure. 7. Photographic appearance of PLA-PVA porous mat.

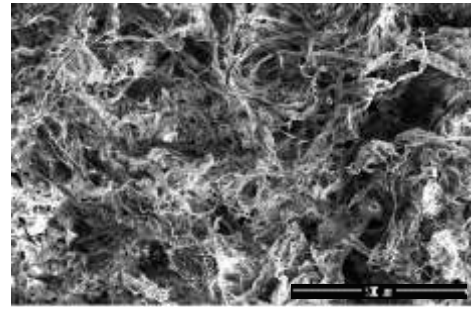


Figure. 8. SEM image of PLA-PVA porous mat

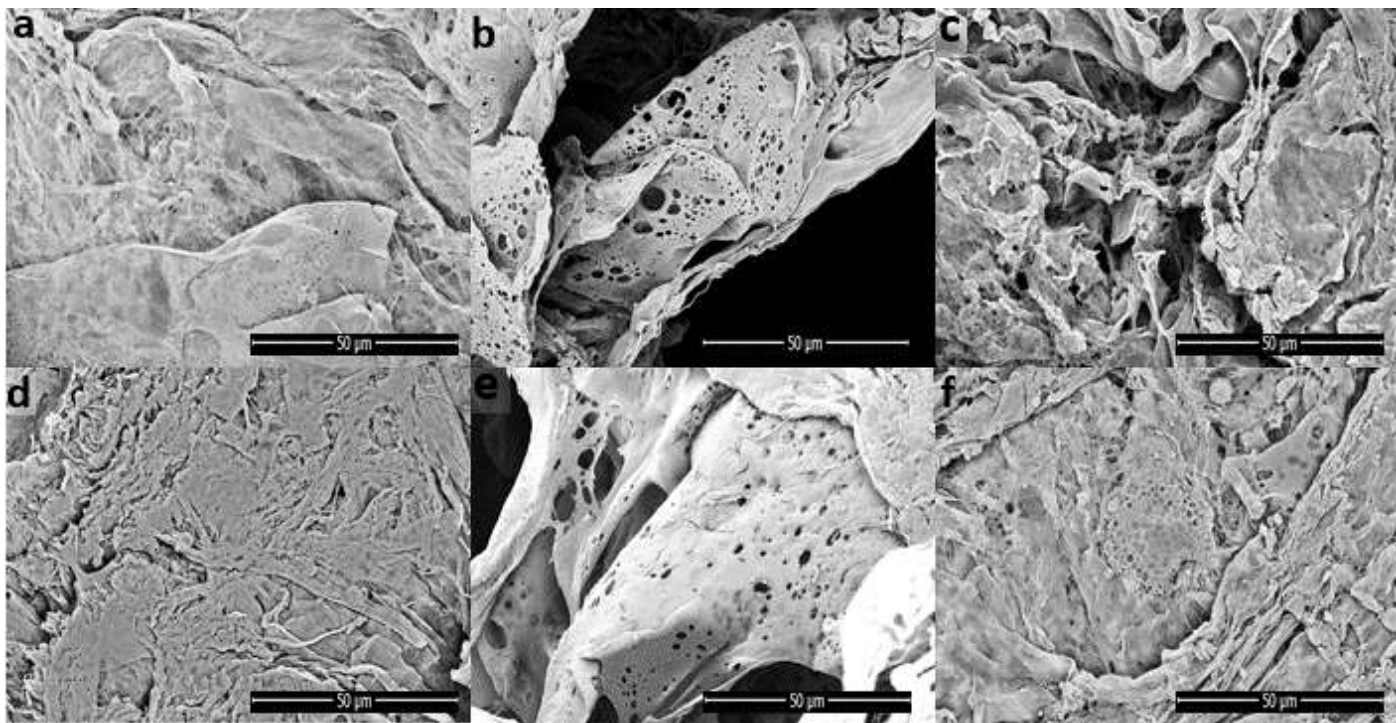


Figure. 9. SEM images of the porous mats: (a) PLA-PVA, (b) PLA-PVA/NaCl, (c) PLA-PVA/KMnO<sub>4</sub>, (d) PLA-PVA (T), (e) PLA-PVA/NaCl (T), and (f) PLA-PVA/KMnO<sub>4</sub> (T).

### Swelling test

The degree of swelling is mainly dependent on the porosity and hydrophilicity of the mats[43, 44]. This property of the mats plays an important role in acceleration of wound healing as it absorbs exudates and fluids secreted from the wound and provides a moist environment in the wound area[45, 46]. Figure. 10 shows the swelling behaviour of the mats. It was observed that increasing porosity led to an

increase in the swelling degree. The highest swelling degree obtained by the non-thermal treated PLA-PVA/NaCl mat. This can be attributed to the high porosity percentage of PLA-PVA/NaCl compared to other mats (Table. 7). The lowest swelling degree was obtained from thermal treated neat PLA-PVA mat due to its lowest porosity and relative high crystallinity[47]. The higher swelling degree of thermal treated PLA-PVA/KMnO<sub>4</sub> mat compared to non-thermal treated PLA-PVA/KMnO<sub>4</sub> mat may be attributed to the formation of carboxylic acid group by oxidation of PVK in the presence of KMnO<sub>4</sub> at an elevated temperature (80°C). Therefore, the higher swelling degree of thermal treated PLA-PVA/KMnO<sub>4</sub> mat is attributed to the higher polarity and hydrophilic character of the carboxylic acid[36, 48, 49].

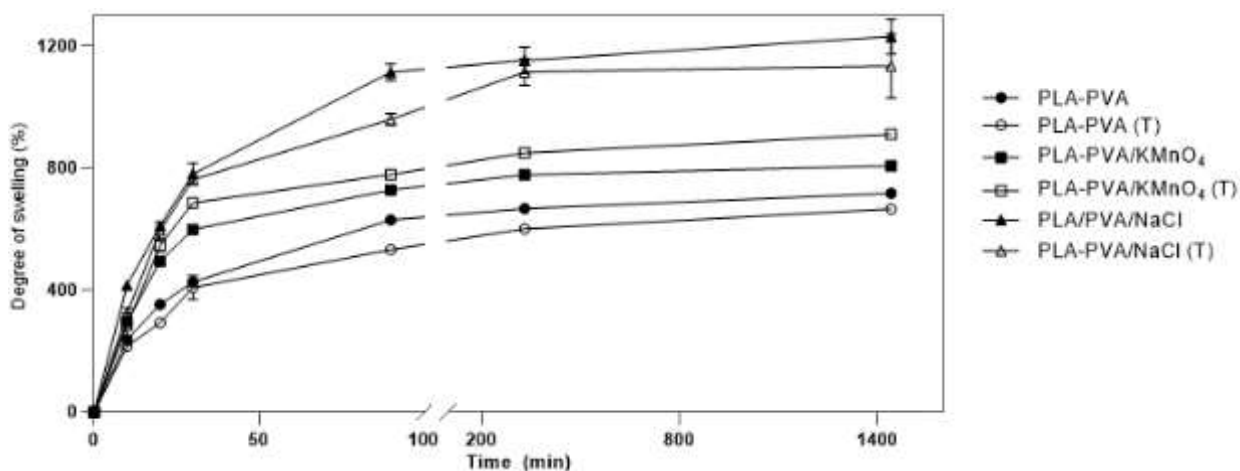


Figure. 10. Swelling studies of the porous mats in PBS with pH 7.4 at 37°C.

## Water solubility

The water solubility of a polymer is a key factor in wound dressing applications, as the rate of degradation or hydrolysis takes place simultaneously with the wound healing process. If the degradation of the wound dressing occurs before the completion of the wound healing process, the wound dressing will need to be applied on the patient several times. This will not only cause discomfort but will also impose extra costs on the patient [50]. The water solubility assessment was performed by calculating the weight loss of the mats in DI water after 24 h. Water solubility of the mats ranges from 2% for thermal treated PLA-PVA and 10% for non-thermal treated PLA-PVA/NaCl as indicated in Table. 8. These results reveal that water solubility increases by increasing the amount of the salts in the mats. This increase in water solubility can be attributed to an increase in the porosity of the mats by the addition

of salts. More porous structures allow and retain a higher number of water molecules in their structure [50, 51]. It is worth noting that all the mats kept their initial shape even after 24 h. Notably, the thermal treatment of the mats did not significantly affect the values of water solubility.

Table. 8. Water solubility measurements of the porous mats in DI water after 24 h at 37°C.

	Untreated			After thermal treatment		
Sample	PLA-PVA	PLA-PVA/KMnO <sub>4</sub>	PLA-PVA/NaCl	PLA-PVA	PLA-PVA/KMnO <sub>4</sub>	PLA-PVA/NaCl
Water solubility	4.09±0.00	6.50±0.20	10.87±0.18	2.67±0.25	7.36±0.18	9.41±0.50

### Water vapour transmission rate (WVTR)

Water vapour transmission rate is the measurement of the amount of water lost through the dressing material [37]. An ideal wound dressing material should protect the wound from dehydration, which will occur due to high WVTR. It should also protect the wound from accumulation of exudate and the risk of bacterial growth caused by low WVTR [52, 53]. To maintain a moist environment for better wound healing the optimal range of WVTR for wound dressing material is 2000 - 2500 (g/m<sup>2</sup>.day) [54, 55]. As shown in Table. 9, the measured value WVTR of the mats were in the range of 2115 - 2287 g/m<sup>2</sup>.day. As previously mentioned, the addition of salts increased the porosity of the mats. This increase in the porosity is the main reason for the observed increase in values of the WVTR in PLA-PVA/NaCl and PLA-PVA/KMnO<sub>4</sub> mats. The thermal treatment of the mats did not affect the values of WVTR. The obtained WVTR results demonstrate that the mats are suitable for wound dressing applications [54, 55].

Table. 9. Water vapour transmission rate of the porous mats.

	Untreated			After thermal treatment		
Sample	PLA-PVA	PLA-PVA/KMnO <sub>4</sub>	PLA-PVA/NaCl	PLA-PVA	PLA-PVA/KMnO <sub>4</sub>	PLA-PVA/NaCl
WVTR	2146.01±19.48	2214.16±20.94	2287.61±25.31	2077±18.65	2207.08±24.45	2259.3±21.35

### In-vitro drug release studies

An ideal antimicrobial wound dressing should sustain a long period of controlled drug release in order to accelerate the healing process and to avoid frequent changing of the dressing [29]. Gentamicin sulfate as an antibiotic agent was loaded into the PLA-PVA mats. The effect of the addition of different types of salts and thermal treatment on entrapment efficiency (EE), loading capacity (LC), and in-vitro were studied. Tang *et al.* reported that the EE of drugs in the surface liquid spraying method is higher than the EE of drugs in traditional emulsion solvent evaporation method [56]. Therefore, liquid spraying method was used to obtain a higher EE. As shown in Table. 10, the surface liquid spraying method resulted in a high entrapment efficiency of the drug (90.11%). Furthermore, the addition of salts increased the EE. This could be attributed to changing the aqueous solubility of the organic solvent by salt [57, 58]. This could also be explained by increasing the porosity of the mats due to the addition of salts as mentioned in the porosity measurement section [38, 59]. While the thermal treatment did not significantly impact the EE, this was not the case for the PLA-PVA/NaCl. This could be attributed to the reduced porosity of PLA-PVA/NaCl due to the thermal treatment. Table 10 demonstrates that the addition of salts and thermal treatment did not affect LC (%), which can be attributed to the strong dependency of LC on the polymer weight ratio.

Table. 10. EE and LC of the porous mats before and after thermal treatment.

	Untreated treatment			After thermal treatment		
	PLA-PVA	PLA-PVA/KMnO <sub>4</sub>	PLA-PVA/NaCl	PLA-PVA	PLA-PVA/KMnO <sub>4</sub>	PLA-PVA/NaCl
<b>EE (%)</b>	90.11±0.21	92.08±0.06	97.57±0.03	92.38±0.49	93.52±0.46	86.7±0.4
<b>LC (%)</b>	4.5±0.01	4.6±0.003	4.8±0.001	4.6±0.02	4.7±0.02	4.32±0.02

The addition of salts to the polymer has a crucial effect on the initial burst release and the porosity of the mats. The initial burst release and the porosity of the mats varies depending on the salt concentration [38]. The in-vitro release profiles of antibiotics from the wound dressings are displayed in Figure. 11. PLA-PVA/NaCl mat exhibited the highest initial burst release due to the highest salt concentration and porosity. The cumulative drug release was around 82 %. The burst release rate during the first 24 hours in PLA-PVA/NaCl mat can be attributed to the fact that the aqueous environment washed all the drug from the surface and other nearby drug and was removed through the pores of the polymer matrix [59, 60]. In comparison with PLA-PVA/NaCl mat, thermal treated PLA-PVA/NaCl mat, showed an initial burst release of drugs during the first 6 hours of around 11%. This clearly showed a reducing initial burst release followed by a gradual release in a decreasing rate over time with around 50% release of the drug during 14 days. These results are consistent with the results of other groups where thermal treatment was employed as a tool for prolonging the release of the drug. Moreover, thermal treatment of polymer at temperatures above  $T_g$  reduced the drug release rate [61, 62]. This can be attributed to the fact that thermal treatment increases the crystallinity of the polymer, in which crystalline domains function as a physical barrier, leading to slower diffusion of the drug [31]. As a result, thermal treatment of the PLA-PVA/NaCl mat causes the sustained release of GS. However due to the heating of the mats above  $T_g$  (80°C) the drug release rate was reduced.

As shown in Figure. 11, for PLA-PVA/KMnO<sub>4</sub> mat, the initial burst release of drugs during the first 24 hours was only approximately 20%, followed by a gradual and constant release of GS over 14 days. The cumulative drug release was 33%. However, thermal treated PLA-PVA/KMnO<sub>4</sub> mat showed an initial burst release of around 12 % during the first 6 hours followed by a fast sustained release profile around 61% over 14 days. As can be seen in the Figure, the cumulative drug release rate of heat treated PLA-PVA/KMnO<sub>4</sub> mat had a higher release rate in comparison

with PLA-PVA/KMnO<sub>4</sub> mat. This could be explained by the formation of PVK as the result of the interaction between KMnO<sub>4</sub> and PVA. Thermal treatment of PLA-PVA/KMnO<sub>4</sub> mat caused partial oxidation of the formed PVK by KMnO<sub>4</sub>, and as a result formation of carboxylic acid groups. Carboxylic acids have a higher polarity and hydrophilic character in comparison with ketones (PVK) [36, 48, 49]. Therefore, thermally treated PLA-PVA/KMnO<sub>4</sub> mat have a relatively higher hydrophilicity as compared to non-thermal treated PLA-PVA/KMnO<sub>4</sub> mat. This higher hydrophilicity causes PBS to permeate more freely into thermal treated PLA-PVA/KMnO<sub>4</sub> mat than it can permeate into the PLA-PVA/KMnO<sub>4</sub> mat. Hence, although thermal treatment of the PLA-PVA/KMnO<sub>4</sub> mat led to a decrease in the porosity, its higher relative hydrophilic character caused the higher cumulative release rate.

For the neat PLA-PVA mat, the initial burst release occurred during the first 6 hours followed by a slow and gradual release at around 58% over 14 days (Figure. 11). The thermally treated neat PLA-PVA mat exhibited the initial burst release in the first 6 hours at around 14% and the cumulative drug release was 20%. This means that the thermally treated neat PLA-PVA mat could not release the drugs and kept the drug inside the mat. This can be attributed to the less porous structure and relatively higher crystallinity of the mat [63].

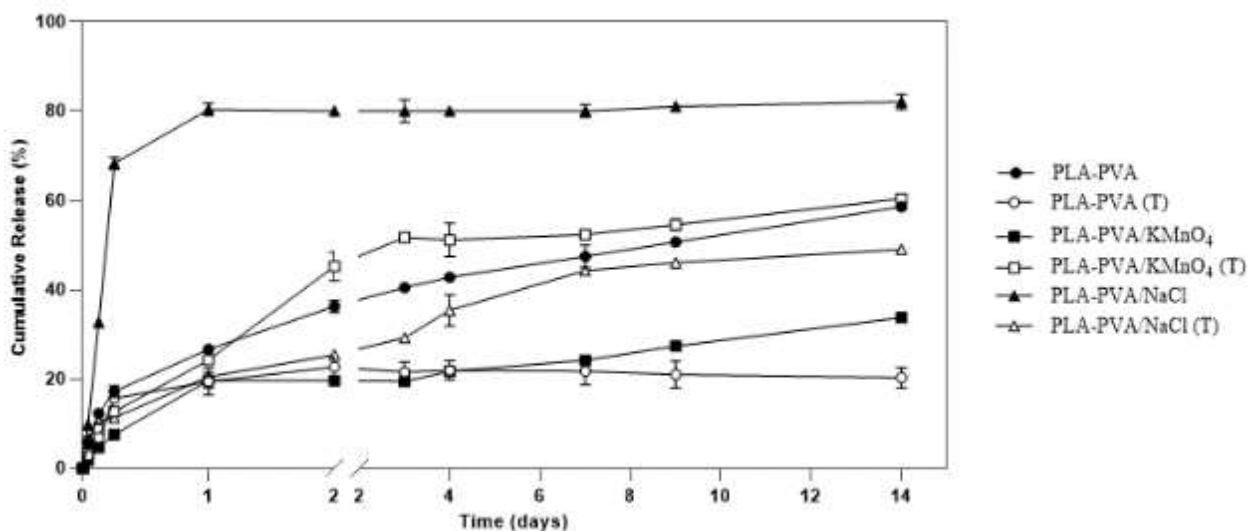


Figure. 11. In-vitro release profiles of porous mats loaded GS in pH 7.4 at 37°C.



## CONCLUSIONS

Polymeric porous mats of PLA-PVA were prepared in this study by a slightly modified form of surface liquid spraying method. The effects of the addition of different salts (NaCl and  $\text{KMnO}_4$ ) and thermal treatment (80 °C for 2 min) on the mats were investigated. The SEM results indicated that prepared mats had interconnected porous structures and the addition of salts considerably enhanced the porosity of the mats. Moreover, the swelling degree and water solubility of mats were increased due to the increase in porosity. The in-vitro release of gentamicin sulfate was studied and it was shown that a higher entrapment efficiency and initial burst release was achieved by the addition of salt to the aqueous phase. Additionally, the thermal treatment of the polymer above  $T_g$  reduced the initial burst release and prolonged the release of the drug. Finally, it worth noting that the procedure suggested in this study to prepare mats is cost-efficient and non-toxic, since all the solvents can be easily and completely removed. Therefore, the novel PLA-PVA mats developed in this work could be a potential candidate for wound dressing applications in the future.

## SUMMARY OF WORK

Polyesters are widely used biodegradable polymers in biomedical applications such as drug delivery, cancer therapy, wound dressing, surgical use, and more. However, due to their intrinsic properties, such as hydrophobicity, polyesters should be modified in order to fine tune their use in some applications. Poly (lactic acid) is an environmentally-friendly polyester that has drawn attention over the past few decades owing to its suitable biocompatible, biodegradable and bioactive properties. PLA is highly hydrophobic polymer, therefore, one approach to address this issue is blending with another material to make porous structure. In this way porosity is increased and this in turn, increases the contact surface of the polymer.

According to the current state of knowledge, the overview of hydrophobic issue was drawn in the theoretical part, and research aims of work were defined. On the basis of this, the experimental part was devoted to the preparation of different PLA-based porous system for biomedical applications.

In this thesis, the first project focused on preparing and characterizing antibacterial, microcellular polymeric material based on PLA, utilizing potassium aluminium sulfate dodecahydrate (ALUM) as an antimicrobial agent and monobasic sodium salts as a blowing agent. Morphological analysis of the surface of specimens revealed that adding ALUM instigated greater cell density in the polymer matrix and reduced average cell size. The results showed increasing porosity in the polymer matrix led to an increase in release of ALUM. Moreover, porous samples showed effective antimicrobial activity against *E. coli* in comparison with *S. aureus*.

In the second project polymeric porous mats of PLA-PVA were prepared by surface liquid spraying technique. The SEM results indicated that mats had interconnected porous structures and the addition of salts considerably enhanced the porosity of the mats. The in-vitro release of gentamicin sulfate was studied and it was shown that a higher entrapment efficiency was achieved by the addition of salt to the aqueous phase.

## REFERENCES

1. Richbourg, N.R., N.A. Peppas, and V.I. Sikavitsas, *Tuning the Biomimetic Behavior of Scaffolds for Regenerative Medicine Through Surface Modifications*. Journal of tissue engineering and regenerative medicine, 2019.
2. Sevim, K., *Modelling of Drug Release from Biodegradable Polymers*. 2017, Department of Engineering.
3. Albertsson, A.-C. and I.K. Varma, *Aliphatic polyesters: synthesis, properties and applications*, in *Degradable Aliphatic Polyesters*. 2002, Springer. p. 1-40.
4. Russell, J., *A General Approach Towards the Synthesis of Amido-Functionalized Biodegradable Polyesters*. 2010.
5. Gigli, M., et al., *Poly (butylene succinate)-based polyesters for biomedical applications: A review*. European Polymer Journal, 2016. **75**: p. 431-460.
6. Castro-Aguirre, E., et al., *Poly(lactic acid)—Mass production, processing, industrial applications, and end of life*. Advanced Drug Delivery Reviews, 2016. **107**: p. 333-366.
7. Liu, L., et al., *Preparation of Antimicrobial Membranes: Coextrusion of Poly(lactic acid) and Nisaplin in the Presence of Plasticizers*. Journal of Agricultural and Food Chemistry, 2009. **57**(18): p. 8392-8398.
8. Stloukal, P., et al., *The influence of a hydrolysis-inhibiting additive on the degradation and biodegradation of PLA and its nanocomposites*. Polymer Testing, 2015. **41**: p. 124-132.
9. Zhao, H., et al., *Morphology and Properties of Injection Molded Solid and Microcellular Poly(lactic acid)/Poly(hydroxybutyrate-Valerate (PLA/PHBV) Blends*. Industrial & Engineering Chemistry Research, 2013. **52**(7): p. 2569-2581.
10. Matuana, L.M., *Solid state microcellular foamed poly(lactic acid): Morphology and property characterization*. Bioresource Technology, 2008. **99**(9): p. 3643-3650.
11. Pan, J., *5 - Modelling biodegradation of composite materials made of biodegradable polyesters and tricalcium phosphates (TCPs)*, in *Modelling Degradation of Bioresorbable Polymeric Medical Devices*, J. Pan, Editor. 2015, Woodhead Publishing. p. 71-87.
12. Pilla, S., et al., *Microcellular extrusion foaming of poly(lactide)/poly(butylene adipate-co-terephthalate) blends*. Materials Science and Engineering: C, 2010. **30**(2): p. 255-262.
13. Stloukal, P., et al., *Carbodiimide additive to control hydrolytic stability and biodegradability of PLA*. Polymer Testing, 2016. **54**: p. 19-28.
14. Kucharczyk, P., et al., *Novel aspects of the degradation process of PLA based bulky samples under conditions of high partial pressure of water vapour*. Polymer Degradation and Stability, 2013. **98**(1): p. 150-157.
15. Lu, L., et al., *In vitro degradation of porous poly(l-lactic acid) foams*. Biomaterials, 2000. **21**(15): p. 1595-1605.
16. Kim, J.S., et al., *Antimicrobial effects of silver nanoparticles*. Nanomedicine: Nanotechnology, Biology and Medicine, 2007. **3**(1): p. 95-101.
17. Sondi, I. and B. Salopek-Sondi, *Silver nanoparticles as antimicrobial agent: a case study on E. coli as a model for Gram-negative bacteria*. Journal of Colloid and Interface Science, 2004. **275**(1): p. 177-182.
18. Gupta, D. and A. Laha, *Antimicrobial activity of cotton fabric treated with Quercus infectoria extract*. 2007.

19. Panagiotis, D., et al., *Cornet-Like Phosphotriazine/Diamine Polymers as Reductant and Matrix for the Synthesis of Silver Nanocomposites with Antimicrobial Activity*. *Macromolecular Materials and Engineering*, 2010. **295**(2): p. 108-114.
20. CORRAL, L.G., L.S. POST, and T.J. MONTVILLE, *Antimicrobial Activity of Sodium Bicarbonate: A Research Note*. *Journal of food science*, 1988. **53**(3): p. 981-982.
21. Liu, Y., et al., *Simultaneous Enhancement of Strength and Toughness of PLA Induced by Miscibility Variation with PVA*. *Polymers*, 2018. **10**(10): p. 1178.
22. Li, T.-T., et al., *Manufacture and characteristics of HA-Electrodeposited polylactic acid/polyvinyl alcohol biodegradable braided scaffolds*. *Journal of the Mechanical Behavior of Biomedical Materials*, 2020. **103**: p. 103555.
23. Li, T.-T., et al., *Properties and Mechanism of Hydroxyapatite Coating Prepared by Electrodeposition on a Braid for Biodegradable Bone Scaffolds*. *Nanomaterials*, 2019. **9**(5): p. 679.
24. Abdullah, O.G., S.B. Aziz, and M.A. Rasheed, *Structural and optical characterization of PVA:KMnO<sub>4</sub> based solid polymer electrolyte*. *Results in Physics*, 2016. **6**: p. 1103-1108.
25. Hassan, R.M. and M.A. Abd-Alla, *New coordination polymers. Part 1.—Novel synthesis of poly (vinyl ketone) and characterization as chelating agent*. *Journal of Materials Chemistry*, 1992. **2**(6): p. 609-611.
26. Ali, H.E., *A novel optical limiter and UV–Visible filters made of Poly (vinyl alcohol)/KMnO<sub>4</sub> polymeric films on glass-based substrate*. *Journal of Materials Science: Materials in Electronics*, 2019. **30**(7): p. 7043-7053.
27. Dai, L., et al., *Gelation of a new hydrogel system of atactic-poly(vinyl alcohol)/NaCl/H<sub>2</sub>O*. *Polymer International*, 2002. **51**(8): p. 715-720.
28. Yang, H., et al., *Thermal decomposition behavior of poly (vinyl alcohol) with different hydroxyl content*. *Journal of Macromolecular Science, Part B*, 2012. **51**(3): p. 464-480.
29. Zhang, D., et al., *Carboxyl-modified poly(vinyl alcohol)-crosslinked chitosan hydrogel films for potential wound dressing*. *Carbohydrate Polymers*, 2015. **125**: p. 189-199.
30. Doménech-Carbó, M.T., et al., *Study of ageing of ketone resins used as picture varnishes by FTIR spectroscopy, UV–Vis spectrophotometry, atomic force microscopy and scanning electron microscopy X-ray microanalysis*. *Analytical and Bioanalytical Chemistry*, 2008. **391**(4): p. 1351-1359.
31. Castro, A.G.B., et al., *Incorporation of simvastatin in PLLA membranes for guided bone regeneration: effect of thermal treatment on simvastatin release*. *Rsc Advances*, 2018. **8**(50): p. 28546-28554.
32. Omelczuk, M.O. and J.W. McGinity, *The Influence of Thermal Treatment on the Physical-Mechanical and Dissolution Properties of Tablets Containing Poly(DL-Lactic Acid)*. *Pharmaceutical Research*, 1993. **10**(4): p. 542-548.
33. Yin, H.-M., et al., *Engineering Porous Poly(lactic acid) Scaffolds with High Mechanical Performance via a Solid State Extrusion/Porogen Leaching Approach*. *Polymers*, 2016. **8**(6): p. 213.
34. Sabino, M.A., *Oxidation of polycaprolactone to induce compatibility with other degradable polyesters*. *Polymer Degradation and Stability*, 2007. **92**(6): p. 986-996.
35. Stocco, E., et al., *Partially oxidized polyvinyl alcohol as a promising material for tissue engineering*. *Journal of tissue engineering and regenerative medicine*, 2017. **11**(7): p. 2060-2070.
36. Ranganath, M., R.V. Patil, and B. Lobo. *Morphological modifications in potassium permanganate doped poly (vinyl alcohol) films*. in *Proceedings of the International Workshop on Applications of Nanotechnology to Energy, Environment and Biotechnology (NANOEEB)*. 2010.
37. Poonguzhali, R., S.K. Basha, and V.S. Kumari, *Novel asymmetric chitosan/PVP/nanocellulose wound dressing: In vitro and in vivo evaluation*. *International journal of biological macromolecules*, 2018. **112**: p. 1300-1309.

38. K. F. Pistel, T.K., *Effects of salt addition on the microencapsulation of proteins using W/O/W double emulsion technique*. Journal of Microencapsulation, 2000. **17**(4): p. 467-483.
39. Billa, N., K.-H. Yuen, and K.-K. Peh, *Diclofenac Release from Eudragit-Containing Matrices and Effects of Thermal Treatment*. Drug Development and Industrial Pharmacy, 1998. **24**(1): p. 45-50.
40. Azarmi, S., et al., *Thermal treating as a tool for sustained release of indomethacin from Eudragit RS and RL matrices*. International Journal of Pharmaceutics, 2002. **246**(1): p. 171-177.
41. Hasanzadeh, D., et al., *Thermal Treating of Acrylic Matrices as a Tool for Controlling Drug Release*. Chemical and Pharmaceutical Bulletin, 2009. **57**(12): p. 1356-1362.
42. Ungaro, F., et al., *Cyclodextrins in the production of large porous particles: Development of dry powders for the sustained release of insulin to the lungs*. European Journal of Pharmaceutical Sciences, 2006. **28**(5): p. 423-432.
43. Archana, D., J. Dutta, and P.K. Dutta, *Evaluation of chitosan nano dressing for wound healing: Characterization, in vitro and in vivo studies*. International Journal of Biological Macromolecules, 2013. **57**: p. 193-203.
44. Gonzaga, V.d.A.M., et al., *Chitosan-laponite nanocomposite scaffolds for wound dressing application*. Journal of Biomedical Materials Research Part B: Applied Biomaterials, 2020. **108**(4): p. 1388-1397.
45. Lin, Z., et al., *Biofunctions of antimicrobial peptide-conjugated alginate/hyaluronic acid/collagen wound dressings promote wound healing of a mixed-bacteria-infected wound*. International Journal of Biological Macromolecules, 2019. **140**: p. 330-342.
46. Gomaa, S.F., et al., *New polylactic acid/ cellulose acetate-based antimicrobial interactive single dose nanofibrous wound dressing mats*. International Journal of Biological Macromolecules, 2017. **105**: p. 1148-1160.
47. Pantani, R. and A. Sorrentino, *Influence of crystallinity on the biodegradation rate of injection-moulded poly(lactic acid) samples in controlled composting conditions*. Polymer Degradation and Stability, 2013. **98**: p. 1089-1096.
48. Ivanets, A.I., et al., *Physicochemical properties of manganese oxides obtained via the sol-gel method: The reduction of potassium permanganate by polyvinyl alcohol*. Russian Journal of Physical Chemistry A, 2017. **91**(8): p. 1486-1492.
49. McMurry, J.E., *Organic Chemistry*. 2015: Cengage Learning.
50. Koosehgo, S., et al., *Preparation and characterization of in situ chitosan/polyethylene glycol fumarate/thymol hydrogel as an effective wound dressing*. Materials Science and Engineering: C, 2017. **79**: p. 66-75.
51. Kavoosi, G., S.M.M. Dadfar, and A.M. Purfard, *Mechanical, physical, antioxidant, and antimicrobial properties of gelatin films incorporated with thymol for potential use as nano wound dressing*. Journal of Food Science, 2013. **78**(2): p. E244-E250.
52. Akhavan-Kharazian, N. and H. Izadi-Vasafi, *Preparation and characterization of chitosan/gelatin/nanocrystalline cellulose/calcium peroxide films for potential wound dressing applications*. International journal of biological macromolecules, 2019. **133**: p. 881-891.
53. Alippilakkotte, S., S. Kumar, and L. Sreejith, *Fabrication of PLA/Ag nanofibers by green synthesis method using Momordica charantia fruit extract for wound dressing applications*. Colloids and Surfaces A: Physicochemical and Engineering Aspects, 2017. **529**: p. 771-782.
54. Khorasani, M.T., et al., *Incorporation of ZnO nanoparticles into heparinised polyvinyl alcohol/chitosan hydrogels for wound dressing application*. International journal of biological macromolecules, 2018. **114**: p. 1203-1215.
55. Adeli, H., M.T. Khorasani, and M. Parvazinia, *Wound dressing based on electrospun PVA/chitosan/starch nanofibrous mats: Fabrication, antibacterial and cytocompatibility*

- evaluation and in vitro healing assay*. International journal of biological macromolecules, 2019. **122**: p. 238-254.
56. Tang, H., et al., *Application of a novel approach to prepare biodegradable polylactic-co-glycolic acid microspheres: Surface liquid spraying*. Yakugaku Zasshi, 2007. **127**(11): p. 1851-1862.
  57. Dinarvand, R., et al., *Effect of surfactant HLB and different formulation variables on the properties of poly-D,L-lactide microspheres of naltrexone prepared by double emulsion technique*. Journal of Microencapsulation, 2005. **22**(2): p. 139-151.
  58. Al-Maaieh, A. and D.R. Flanagan, *Salt and cosolvent effects on ionic drug loading into microspheres using an O/W method*. Journal of Controlled Release, 2001. **70**(1): p. 169-181.
  59. Al-Sokanee, Z.N., et al., *The Drug Release Study of Ceftriaxone from Porous Hydroxyapatite Scaffolds*. AAPS PharmSciTech, 2009. **10**(3): p. 772-779.
  60. Zare, M., et al., *Effect of additives on release profile of leuprolide acetate in an in situ forming controlled-release system: In vitro study*. Journal of Applied Polymer Science, 2008. **107**(6): p. 3781-3787.
  61. Javadzadeh, Y., L. Musaalrezaei, and A. Nokhodchi, *Liquisolid technique as a new approach to sustain propranolol hydrochloride release from tablet matrices*. International Journal of Pharmaceutics, 2008. **362**(1): p. 102-108.
  62. Azarmi, S., et al., *Mechanistic evaluation of the effect of thermal-treating on Eudragit RS matrices*. Il Farmaco, 2005. **60**(11): p. 925-930.
  63. Tamboli, V., G.P. Mishra, and A.K. Mitra, *Novel pentablock copolymer (PLA-PCL-PEG-PCL-PLA)-based nanoparticles for controlled drug delivery: effect of copolymer compositions on the crystallinity of copolymers and in vitro drug release profile from nanoparticles*. Colloid and Polymer Science, 2013. **291**(5): p. 1235-1245.

## LIST OF FIGURES

Figure 1. Scheme of Surface liquid spraying process .....	11
Figure 2. SEM micrographs of the microstructures of (A) PLA, (B) PLA-ALUM, (C) PLA/MSS3, (D) PLA/MSS5, (E) PLA/ALUM/MSS3, (F) PLA/ALUM/MSS..15	
Figure. 3. Molecular weight evolution of the materials during abiotic hydrolysis ....	18
Figure. 4. Release of ALUM in phosphate buffer saline (PBS) buffer (pH = 7.4) at 37°C .....	21
Figure. 5. FT-IR spectra of PLA-PVA (a), PLA-PVA (T) (b), PLA-PVA/KMnO <sub>4</sub> (c), PLA-PVA/KMnO <sub>4</sub> (T) (d), PLA-PV/NaCl (e), PLA-PVA/NaCl (T) (f) mats .....	22
Figure. 6. DSC curves of porous PLA mats .....	24
Figure. 7. Photographic appearance of the PLA-PVA porous mat .....	26
Figure. 8. SEM image of PLA-PVA porous mat .....	26
Figure. 9. SEM images of the porous mats: (a) PLA-PVA, (b) PLA-PVA/NaCl, (c) PLA-PVA/KMnO <sub>4</sub> , (d) PLA-PVA (T), (e) PLA-PVA/NaCl (T), and (f) PLA-PVA/KMnO <sub>4</sub> (T) .....	29
Figure. 10. Swelling studies of the porous mats in PBS with pH 7.4 at 37°C.....	27
Figure. 11. In-vitro release profiles of porous mats loaded GS in pH 7.4 at 37°C.....	31

## LIST OF TABLES

Table. 1. Compositions of the investigated samples .....	9
Table. 2. Selected material-related properties of samples after preparation and before degradation experiments .....	13
Table. 3. Initial mechanical properties of neat PLA and microcellular PLA .....	14
Table. 4. Thermal properties of samples prior to and after abiotic hydrolysis at various times .....	16
Table. 5. Reduction in colony forming units (CR) effected by of pure PLA-ALUM, microcellular PLA/ALUM/MSS3, and microcellular PLA/ALUM/MSS5 .....	19
Table. 6. Selected material-related properties of the mats before and after thermal treatment .....	23
Table. 7. Porosity measurements of porous mats after 24 h of immersion in ethanol at room temperature .....	25
Table. 8. Water solubility measurements of the porous mats in DI water after 24 h at 37°C .....	28
Table. 9. Water vapor transmission rate of the porous mats .....	29
Table. 10. EE and LC of the porous mats before and after thermal treatment .....	30



# CURRICULUM VITAE

## Contact information

Name: Maliheh Amini Moghaddam

Email: [Amini@utb.cz](mailto:Amini@utb.cz)

Address: T. G. Masaryka 1281, Zlin, Czech Republic.

## Education

- |                  |  |
|------------------|--|
| <b>2016-2021</b> | Ph.D. student at Tomas Bata University, Zlin, Czech Republic.          |
| <b>2010-2013</b> | M.Eng. Chemical Engineering at Azad University, Shahrood Branch, Iran. |
| <b>2004-2010</b> | B.Eng. Chemical Engineering at Azad University, Quchan Branch, Iran.   |

## Significant projects in PhD

- Development and characterization of microcellular antibacterial polylactide-based systems for medical applications.
- Poly lactide-polyvinyl alcohol-based porous systems loaded with gentamicin for wound dressing applications.
- Preparation and characterization of gold nanoclusters stabilized with chitosan and investigation of hyperthermic effects of gold nanoclusters-chitosan composites on cells for cancer therapy
- Preparation and modification of polyclay.
- Conjugated polymers based materials as luminescence chemo sensors.

|

## Research Experience

- 2016-2021                      Doctoral research at Centre of Polymer Systems (CPS), Tomas Bata University, focuses on polymers for medical applications.
- Feb 2019-Aug2019            ‘‘Free mover mobility’’ – Monash University (Australia)  
Preparation and characterization of chitosan functionalized gold nanocluster and investigation of hypothermia effects on cells for cancer therapy application.
- 2016-2020                      Internal Grant Agency of FT TBU, Research team member.

## LIST OF PUBLICATIONS

1. Maliheh Amini Moghaddam, Petr Stloukal, Pavel Kucharczyk, Aneta Tor-Swiatek, Tomasz Garbacz, Martina Pummerová, Tomasz Klepka, Vladimír Sedlařík. *Microcellular antibacterial polylactide-based systems prepared by additive extrusion with ALUM*. *Polymers for Advanced Technologies*, 2019. **30**(8): p. 2100-2108.
2. Maliheh Amini Moghaddam, Antonio Di Martino, Tomáš Šopík, Haojie Fei, Jaroslav Císař, Vladimír Sedlařík. *Poly lactide/Polyvinylalcohol-Based Porous Bioscaffold Loaded with Gentamicin for Wound Dressing Applications*. *Polymers*, 2021. **13**(6): p. 921.
3. Maliheh Amini Moghaddam, Antonio Di Martino, Kadir Ozaltin, Pavel S.Postnikov, Marina E.Trusova, Vladimír Sedlarik. Nanoencapsulation as approach to improve shelf-life and stability of a hydrophilic and hydrophobic vitamin, submitted in *Food Science and Technology*.
4. Maliheh Amini Moghaddam, Ishdeep Kaur, Anna Cifuentes-Rius, Antonio Di Martino, Deepagan Veerasikku Gopal, Vladimír Sedlařík, Nicolas H. Voelcker. Hyperthermic effects of gold nanoclusters-chitosan composite on tumour cells, submitted to *biointerphases*.

### Conference Contribution

1. Maliheh Amini Moghaddam, “Optimization Nano-and Submicro-sized Mesoporous Silica particles with tunable size” *Nanocon*, Brno, Czech Republic, 2017.

# **Functionalized biodegradable co-polyesters for medical applications**

Funkcionalizované biologicky rozložitelné kopolyestery pro lékařské aplikace

Doctoral Thesis Summary

Published by: Tomas Bata University in Zlín,

nám. T. G. Masaryka 5555, 760 01 Zlín.

Edition: published electronically

Typesetting by: Maliheh Amini Moghaddam, Ph.D.

This publication has not undergone any proofreading or editorial review.

Publication year: 2021

First Edition

ISBN 978-80-7678-002-6

